

## Two-dimensional micron-step probe drive for laboratory plasma measurement

A. Collette and W. Gekelman

*Department of Physics and Astronomy, University of California, Los Angeles, 1000 Veteran Ave., Suite 15-70, California 90095, USA*

(Received 9 June 2008; accepted 25 July 2008; published online 25 August 2008)

Laboratory measurement of small-scale ( $\sim 1$  mm) magnetic phenomena over an extended area is a challenge requiring precise diagnostics. We present a novel two dimensional magnetic probe platform capable of directly measuring the magnetic field over a  $36\text{ cm}^2$  region at spatial resolutions better than 1 mm. The platform is discussed in the context of an experiment at the Large Plasma Device facility at UCLA, designed to measure the magnetic interaction between two counterpropagating laser-produced plasmas. The use of a precise, repeatable positioning platform enables the recovery of information about the interaction using cross-correlation techniques.

© 2008 American Institute of Physics. [DOI: [10.1063/1.2972150](https://doi.org/10.1063/1.2972150)]

### I. INTRODUCTION

The expansion and interaction of dense plasmas in the presence of a magnetized background plasma are important in many astrophysical processes, among them coronal mass ejections and the many examples of plasma jets from astrophotography. Turbulence is expected to be present in many such configurations.

We have conducted a series of experiments which involve the collision of two dense laser-produced plasmas within an ambient, highly magnetized background plasma at the UCLA Large Plasma Device (LaPD) laboratory. The laser-produced plasmas form diamagnetic cavities in which a large percentage of the 600 G background magnetic field has been expelled. The large-scale effects of these phenomena, including their effects on the background plasma, have been the subject of multiple experiments at LaPD.<sup>1,2</sup>

Observations of these structures using a fast (3 ns exposure) camera indicate a complicated structure at late times, in addition to coherent corrugated structures at the cavity boundaries. The data hint at the presence of turbulence in the interaction. Previous measurements of magnetic field fluctuations associated with these events have been limited by the size of probes available and by the manner in which the experiment is performed. The complex structures observed by photography are at most a few millimeters in size. However, the smallest conventional magnetic loop probe at LaPD is approximately 3 mm in diameter and has a positioning accuracy of only  $\pm 3$  mm.

Additionally, as the LaPD is a 1 Hz discharge device, spatially resolved data are usually collected from a series of measurements by a small number of movable probes, which are repositioned inside the vacuum vessel between shots to construct a grid of data points. While this works excellently for repeatable, phase-locked phenomena, it breaks down in the case of turbulent behavior, which although repeatable in character cannot be reconstructed from a collection of single-point measurements. Correlation techniques, which record

the magnetic field behavior at multiple positions simultaneously, have previously<sup>3</sup> been used to recover information about turbulent phenomena using only a few movable probes.

Therefore, in order to investigate turbulent behavior in this experiment, a new measurement technique is needed which (1) can perform magnetic field measurements with spatial resolution equal to or better than 1 mm both in terms of probe size and positioning accuracy and (2) supports measurements from more than one probe, separated by a known, variable distance. To this end, we have developed a novel diagnostic system composed of two small (1 mm) three-axis differential magnetic field probes, one of which is driven by an in-vacuum ceramic motor system capable of extremely fine (100  $\mu\text{m}$ ) positioning accuracy.

### II. DESIGN OVERVIEW

Figure 1 shows the microprobe system as implemented at LaPD. It is a two-axis positioning system capable of locating a probe head with better than 100  $\mu\text{m}$  accuracy in a  $6 \times 6\text{ cm}^2$  plane (see also Fig. 2).

The fundamental technology behind the drive is a vacuum-compatible ceramic motor system capable of very fine step sizes ( $< 1\ \mu\text{m}$ ). The drive force is provided by a stack of piezoelectric crystals; the stack is attached to a short ceramic stalk which is pressed against a drive track (Fig. 3). The piezostack, when driven by the correct waveform from an amplifier, will translate the drive track by friction. This drive strategy results in a system with an extremely fine step resolution (better than the 10  $\mu\text{m}$  observed), no backlash, and a maximum translation speed of several centimeters per second. In addition, commercially available motors can develop tens of newtons of force, which allows the translation of nontrivial amounts of hardware.

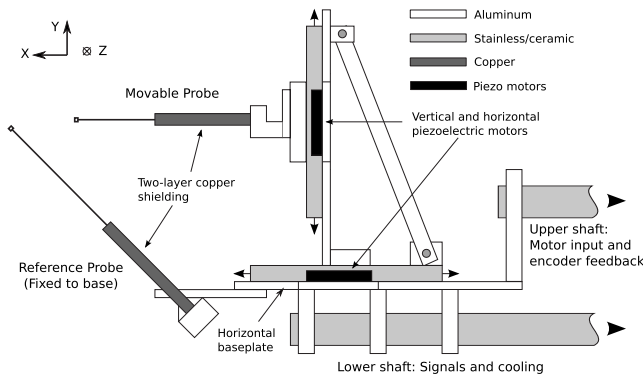


FIG. 1. Overview of the micron-scale probe drive. View is oriented along the axis of the LaPD ( $Z$ ); the drive system is designed to provide access to a 6 cm square region in  $X/Y$ . Not shown are the shields which protect the motors and encoders from direct contact with the background plasma (Fig. 2). Figure 3 shows an overhead view of the drive, with the vertical component removed.

### III. DESIGN CONSTRAINTS

Along with the requirements for positioning accuracy and range, the apparatus is designed around two constraints. First, it must be able to withstand immersion in a 6 eV, 1 Hz,  $10^{12}$  cm $^{-3}$  discharge plasma (10–15 ms lifetime) and a 600–1000 G background magnetic field for several weeks. Second, it must fit through an access port measuring 10 cm wide by 30 cm tall.

The first constraint dictates the use of all nonmagnetic components, along with high-temperature materials where possible. The motors and optical feedback sensors are non-magnetic by design but must be water cooled as they are not necessarily able to withstand the high equilibrium temperature of the motor platform while in the plasma column.

The second constraint requires that the drive geometry conform to a two-dimensional (2D) design, oriented transverse to the background magnetic field. In addition, since the LaPD is designed to operate under vacuum for many months, we further require that the drive be removable even if all axes are in their fully extended state (in case of a mechanical breakdown). The final translation limits are therefore set by the size of the vacuum interlock box and are  $\pm 3$  cm for each axis. The resulting 36 cm $^2$  accessible area provides excellent range, considering the probe head size of 1 mm, and allows a comfortable safety margin.

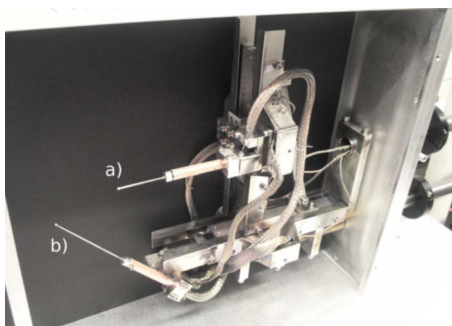


FIG. 2. (Color online) Photograph of the micron-scale probe drive after being immersed for 2 weeks in the LaPD discharge plasma. (a) Movable probe for magnetic field measurements, which can translate in  $X$  and  $Y$  with resolution better than 100  $\mu\text{m}$ . (b) Fixed probe for correlation analysis.

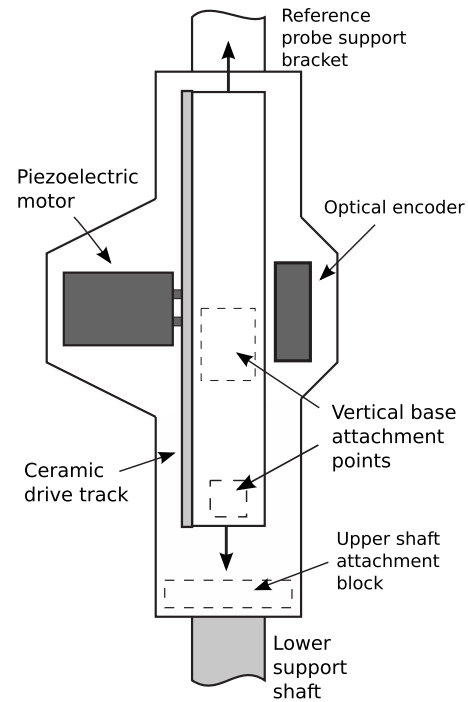


FIG. 3. Baseplate for horizontal drive. The piezoelectric motor at the left pushes on the ceramic drive track, translating the stage. An optical encoder records the position of the assembly. Not shown are stainless steel shields which fit over these components to protect them from the plasma and cooling braids attached to both the motor and encoder (Fig. 2). The vertical drive (see Fig. 1) is mounted within the dashed areas.

### IV. DRIVE DESIGN

#### A. General drive design

Figure 1 shows the design of the 2D probe drive system. The system is built around two aluminum baseplates, each of which supports all hardware necessary for translation of a single axis. Figure 3 shows the horizontal plate. A commercially available translation stage (Small Parts LMS-400/30) is rendered nonmagnetic and vacuum compatible by the replacement of all ferrous components with either stainless steel or ceramic materials; using ceramic ball bearings eliminates the need for lubrication. The stage is attached to the baseplate at two locations. A ceramic drive track is directly attached to one side of the stage with vacuum-compatible adhesive. The piezoelectric motor is pressed against the track with enough force to ensure good coupling of movement and then fixed to the baseplate with four screws.

Two attachment points (dashed outlines in Fig. 3) join the second, vertical-drive baseplate to the midpoint of the horizontal slide. The central attachment point is a solid aluminum block; further reinforcement is provided by an angled brace which connects the top of the vertical baseplate to the end of the slide. The resulting structure resists deformation and vibration caused by movement of the vertical axis.

Motion feedback is provided by an optical encoder (Renishaw RGH-25U) on the opposite side of the stage. A gold-plated tape with hash marks at 20  $\mu\text{m}$  intervals is fixed to the side of the stage in the same manner as the ceramic drive track. An optical read head is positioned 0.8 mm from the tape. This feedback mechanism has a minimum step resolution of 10  $\mu\text{m}$ . To provide additional protection from the

plasma and from carbon blowoff from laser-target experiments in LaPD, the motors, tracks, and encoders are encased in a stainless-steel shield which blocks most of the solid angle from these components to the environment.

The drive platform is suspended inside the plasma on two 1 in. hollow stainless steel shafts. One shaft runs under the horizontal baseplate and is attached to it at three places for maximum stability. The other shaft is attached to a small aluminum extension at the near end of the baseplate. Along with the extra support this provides, the attachment point prevents the platform from rotating about the lower shaft when it is inserted. The vacuum interface at the machine boundary is a double O-ring design with a small central cavity kept at a low (5–10 mtorr) vacuum, which allows the component to slide without admitting air to the high-vacuum side.

In addition to providing mechanical support, all electrical and water connections run through these shafts. Each is capped with a removable flange fitted with vacuum-tight feedthroughs.

## B. Cooling

Because neither the motor nor the encoder is designed to operate continuously at temperatures above 50 °C, active water cooling is required. A 1/8 in. pipe circulating cooling water runs through the lower shaft and ends in a small loop. Flexible copper braid connects the loop to the motors and encoder housings.

## C. Automatic computer control

Because the LaPD is a 1 Hz device, spatially resolved datasets can be easily obtained by collecting an ensemble of shots over many different probe positions. To collect a reasonable number of points, the facility uses an automated computer system to manage probe drives and digitizers. This system is designed in an extensible fashion and supports LABVIEW “modules” which extend the range of devices supported by the system by presenting a common interface for each class of device to the controlling application. For the microprobe platform, a control module was developed which allowed automatic control of the motors over a wireless network link. In addition to the convenience this provides, because the probe drive and associated hardware are immersed in the plasma column and at a significant potential relative to ground, it is also necessary to provide isolation from the rest of the computer system. The result is a fully automated, scriptable drive system which can be operated from anywhere in the private LaPD network.

In addition to recording scientific data, the LaPD automation software records a number of hardware-related state variables for each shot. These include the actual and commanded motor positions, along with the servo “following error” which is a good indicator of mechanical slippage or binding.

## V. DIAGNOSTIC HARDWARE

A three-axis magnetic field probe, with a 1 mm loop head, is attached to an adjustable bracket on the vertical

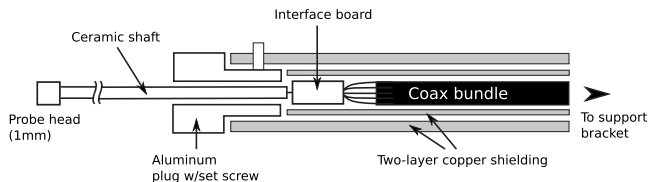


FIG. 4. Magnetic field probe in detail. The probe head is potted in epoxy and attached to the base via a thin (1 mm) ceramic shaft. Magnet wires from the head are attached to coaxial signal lines at a small section of PCB (the “interface board”). To reduce pickup at the connection site, the assembly is double shielded with copper tubing.

slide. Screw-and-slot attachment allows manual offset of the probe position in the vertical and field-aligned ( $Z$ ) directions. In addition to this movable probe, a reference probe of identical construction is attached to the end of the horizontal baseplate. A similar clamp allows adjustment along  $Z$  and a 45° line in the  $X/Y$  plane.

Figure 4 shows a cross section of the movable probe. Each probe axis consists of two loops; they are wound on the head in opposite directions. A differential amplifier subtracts the two signals to arrive at a value proportional to  $dB/dt$ . If there is any electrostatic bias across the probe head, this technique ensures that it does not show up in the final signal. Probe signals are therefore extracted using a total of six small coaxial cables from each head (two for each axis).

The probe head is a 1 mm cube with a total of ten windings per axis (five for each leg of the differential circuit). A 1 mm diameter ceramic stalk (4 cm long for the movable probe, 8 cm for the fixed reference probe) connects the twisted-pair signal wires from the head to an interface board inside a double-shielded section of the copper tube. Six coaxial cables connect to the signal wires and exit the tube through the far end. These are encased in a flexible copper braid to provide protection from the plasma and are brought out through the upper 1 in. probe shaft. Enough slack is provided that both axes can translate freely, without being affected by tension in the signal cable.

Each probe was calibrated using a network analyzer from 100 kHz to 50 MHz. The probe response [ $\sim V_{\text{out}}/(dB/dt)$ ] declined by 40% over that range in a linear fashion in the case of the movable probe and with a rollover beginning at 30 MHz for the fixed probe. This frequency-dependent behavior is accounted for at analysis time.

## VI. PERFORMANCE IN EXPERIMENT

For the colliding plasmas experiment, the system was required to execute repeated data planes within a  $4 \times 4$  cm<sup>2</sup> patch at a variety of step sizes and plane centers. The device was in near-continuous operation for 14 days, executing a move every 1–4 min depending on the number of shots recorded at each point. The smallest step size was 1 mm (the size of the probe head), and the largest following error recorded was 140  $\mu\text{m}$ , which was automatically corrected in subsequent moves. No motion faults occurred over the course of the experiment.

Figure 5 shows a vector plot of magnetic field data measured by the movable probe at a time  $t=660$  ns about half-way through the roughly 1  $\mu\text{s}$  evolution of the diamagnetic

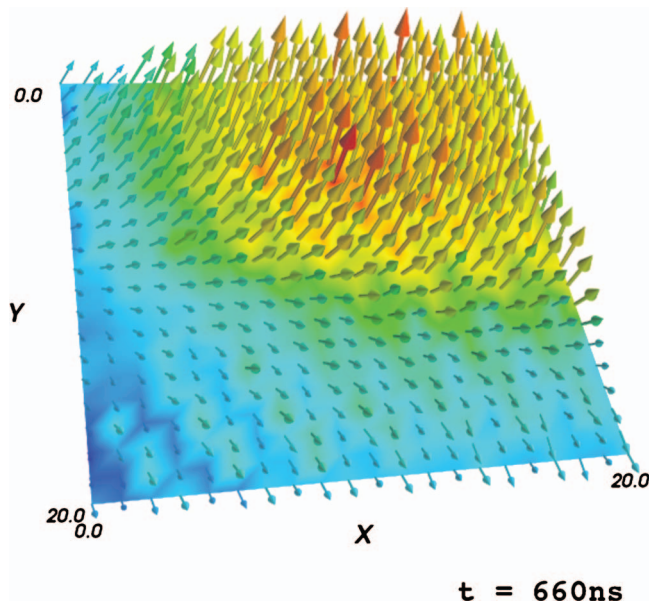


FIG. 5. (Color) Magnetic field measured by the microprobe system about halfway into the  $1 \mu\text{s}$  lifetime of the diamagnetic cavity. The  $X$  and  $Y$  axes are in millimeters. The peak expelled  $B$  field was over 100 G.

cavity. The size of the data patch acquired during this run was  $2 \times 2 \text{ cm}^2$ . This rendering represents the field averaged over many shots and is intended to convey the general structure of the field in the measurement region. The component along  $Z$  corresponds to the expelled field inside the cavities and easily dominates the  $X$  and  $Y$  components. With a background field of 600 G, the excluded field is measured to be over 100 G.

Information on the structure of turbulent behavior can be extracted from the two magnetic field signals via the computation of the cross-spectral function (CSF) an analytic technique which has previously been used to investigate magnetic turbulence in laboratory plasmas.<sup>3</sup> Briefly, if we have an ensemble of  $N$  shots for each spatial position and let  $\Delta\mathbf{r}$  be the vector between fixed and movable probes,  $\Delta t$  be the “lag” (time offset) parameter for the comparison of one trace to another, and  $B_{in1}(\mathbf{r}, t)$  and  $B_{jn2}(\mathbf{r}, t)$  the  $i$ th and  $j$ th components of the magnetic field at the fixed and movable probes, respectively, the CSF is

$$\rho_{ij}(\Delta\mathbf{r}, t, \Delta t) = \frac{1}{A} \frac{1}{N} \sum_{n=0}^N B_{in1}(\mathbf{r}, t) B_{jn2}(\mathbf{r} + \delta\mathbf{r}, t + \Delta t),$$

where  $A$  is a normalization constant.

This object is a nine-element tensor (components  $X_1, Y_1, Z_1$  by components  $X_2, Y_2, Z_2$ ) whose values depend on the probe separation  $\Delta\mathbf{r}$ , the time  $t$ , and the lag  $\Delta t$ . Since we have a spatial grid of coordinates as input, each element of the tensor can be visualized as a plane in  $X/Y$  at a particular time  $t$  and lag  $\Delta t$ . Furthermore, the spatial structure of the laser-plasma interaction should be preserved in the CSF and show up in this plane.

Figure 6 shows the value of this CSF evaluated for components  $B_{x1}$  and  $B_{x2}$ . The spatial region sampled is the same 2 cm patch as Fig. 5, roughly equidistant from the face of

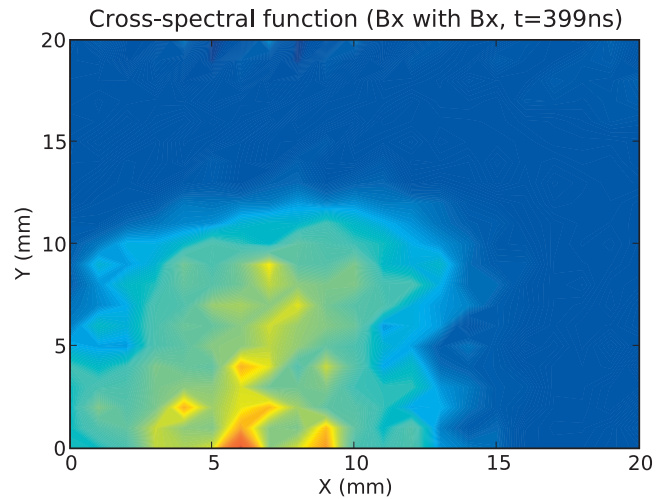


FIG. 6. (Color) Magnitude of the CSF computed for element  $B_x$  against  $B_x$  at lag  $\Delta t=0$ .

each laser target. The general low- $k$  morphology of the structure is preserved. Further processing and analysis in wavenumber space is expected to reveal details of the fine structure.

## VII. SUMMARY AND CONCLUSION

We have designed, tested, and implemented a two-axis probe system to perform measurements of magnetic turbulence with a very fine ( $\sim 1 \text{ mm}$ ) spatial resolution. This system has been fielded at the LaPD, observing structure in the expansion and interaction of two colliding laser-produced plasmas. The device operated continuously while immersed in a 6 eV,  $10^{12} \text{ cm}^{-3}$  discharge plasma for 2 weeks. While data analysis is ongoing, the probe system has collected detailed measurements of the diamagnetic cavity associated with an expanding laser-produced plasma, and the region where turbulence has been observed via photography.

## ACKNOWLEDGMENTS

The authors gratefully acknowledge Marvin Drandell, Zoltan Lucky, and Mio Nakamoto for their invaluable engineering and fabrication work, and Pat Pribyl for the revised design of the magnetic field probe. This project was conducted at the Basic Plasma Science Facility, a national user facility supported by the Department of Energy (DE-FC02-07ER54918), and with a research grant from the National Science Foundation (Phy-0408226). In addition, this research was performed under appointment to the Fusion Energy Sciences Fellowship Program administered by Oak Ridge Institute for Science and Education under Contract No. DE-AC05-06OR23100 between the U.S. Department of Energy and the Oak Ridge Associated Universities.

<sup>1</sup>M. VanZeeland, W. Gekelman, S. Vincena, and J. Maggs, *Phys. Plasmas* **10**, 1243 (2003).

<sup>2</sup>W. Gekelman, A. Collette, and S. Vincena, *Phys. Plasmas* **14**, 062109 (2007).

<sup>3</sup>W. Gekelman and R. L. Stenzel, *J. Geophys. Res.* **89**, 2715 (1984).